

Deep Learning Techniques for Unmixing of Hyperspectral Stimulated Raman Scattering Images

Nikolas Burzynski^{*1}, Yuhao Yuan^{*2}, Adiel Felsen¹, David Reitano¹, Zhibo Wang², Khalid A. Sethi³, fake Lu², and Kenneth Chiu^{1†}

Department of {¹Computer Science, ²Biomedical Engineering},

Binghamton University, State University of New York, Binghamton, NY 13902, USA

³Department of Neurosurgery, United Health Services, Johnson City, NY 13790, USA

^{*}These authors contributed equally

[†]kchiu@binghamton.edu

Abstract—Stimulated Raman Scattering (SRS) microscopy is a stain-free, laser-scanning imaging technology that utilizes two coherent laser beams (i.e., the pump and Stokes) to stimulate vibration of chemical bonds in molecules. Different bonds have different resonant vibrational frequencies, and thus SRS microscopy can achieve rapid chemical imaging at high-resolution, enabling live cell imaging and near-instant, stain-free pathological imaging. To increase the ability to resolve different chemical species, multiple Raman wavenumbers can be used with the hyperspectral SRS imaging data. In particular, this approach holds promise for quantifying DNA content, which is important to characterize cancer cell polyploidy. The SRS spectra is the mixture of the spectra of various pure substances present in each pixel so unmixing must be performed to find the relative abundances of these substances. We ran our SRS hyperspectral data of cancer cells through SciPy’s Least Square Error Linear Optimization algorithm (LSQ) [1] but found that it was not able to return the correct DNA content. Our proposed solution to this problem is to use an autoencoder neural network to unmix the spectra. We based the network on the findings in Palsson et al. (2018) [2]. Our initial results show that the network is effective at finding an accurate linear combination, but the noise in the collection of the SRS hyperspectral data significantly increases the number of low error solutions which makes it difficult for the network to find the true linear combination. Future work will be focused on using noise reduction techniques to help the network find the true abundance values.

I. INTRODUCTION

Current cellular and tissue pathology techniques require chemical staining of the samples and rely on human inspection of the images. This is a slow process that could be made faster using more advanced imaging techniques along with the analytical abilities of neural networks. The imaging technique that we are using in this research is stimulated Raman Scattering (SRS) microscopy [3]. SRS microscopy is a stain-free, laser-scanning imaging technology that utilizes two laser beams (i.e., the pump and Stokes) to stimulate the chemical bond vibration of molecules. Different bonds have different resonant vibrational frequencies, and thus SRS microscopy can provide rapid chemical imaging at high-resolution, enabling live cell imaging and near-instant, stain-free pathology [4].

To increase the ability to resolve different substances, multiple Raman/SRS frequencies can be used, resulting in

hyperspectral Raman/SRS imaging data. The hyperspectral data is a linear mixture of the pure spectra of substances (which we call endmembers) present in the imaged region. For cancer cell imaging, we assume that the spectrum of a single pixel is made up of some amount of proteins, lipids, DNA, and other biomolecular backgrounds. The unmixing of these spectra provides us with the relative concentrations of these defined endmembers, with which we can segment the key cellular structures, including cell body, cell nuclei, and lipid droplets. Our baseline method of unmixing is SciPy’s Least Square Error Optimizer. We found that it was unable to unmixing the data correctly. To tackle this problem, we propose a modified autoencoder neural network [2].

II. METHODOLOGY

A. Collection of Endmember Spectra

Our first task was collecting the endmembers’ pure spectra. We imaged samples of bovine serum albumin (BSA) to represent the protein endmember, oleic acid (OA) to represent the lipid endmember, and purified DNA as the DNA endmember. The background spectrum was obtained by averaging the spectra of all the background pixels in our input image. We then normalized the intensity of these four spectra between 0 and 1 based on the max achieved by all of them. In this way, the relative magnitudes of the spectra are maintained.

B. Collection of hyperspectral SRS images of HeLa cells

HeLa cells were cultured on a coverglass under normal conditions. Cells were chemically fixed and imaged using a lab-built SRS microscope [5]. Hyperspectral SRS imaging data were collected at 40 Raman shifts between 2800 cm^{-1} to 3050 cm^{-1} with an equal wavenumber interval. The image resolution was 1024×1024 . The image dimension was $175 \mu\text{m}$.

C. Unmixing Using SciPy Optimize Package

To create a baseline result which we could compare our results to, we ran our cancer cell hyperspectral image through SciPy’s Least Square Error Linear Optimizer [1]. This optimizer unmixes a pixel spectrum by finding the linear combination of endmember abundances that minimizes the squared error residual. Each pixel’s spectra was normalized between 0

and 1 and then sent through the optimizer. We reconstructed the input hyperspectral image into an RGB image with the coefficient of BSA being the red channel, DNA the green, and OA the blue. The channels were normalized from 0-1 across all pixels of the image.

D. Unmixing Using Modified Autoencoder Neural Network

Our proposed method of unmixing is a modified autoencoder based on the findings in Palsson et al. (2018) [2]. The autoencoder, developed using PyTorch [6], down-samples the 40-dimensional, normalized, input pixel spectrum through 3 leaky relu hidden layers into a 4-node output with a relu activation function. Our custom loss function uses the activation values of the output nodes as the coefficients of a linear combination of the endmembers. The loss is taken to be the mean square error between this reconstructed spectrum and the original input pixel spectrum. This loss is then minimized via gradient descent and back propagation using the Adam Optimizer with a .0005 learning rate. A schematic of the modified autoencoder is shown in Figure 1. We trained the neural network on a 1024×1024 hyperspectral image for 20 epochs, using a batch size of 1024 for ease of testing the network and shuffled the input pixels in an effort to avoid over fitting since we used the same 1024×1024 image as our test data.

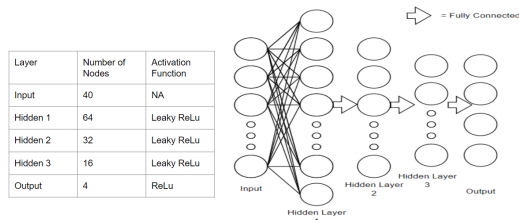


Fig. 1. The modified autoencoder architecture used for this study.

III. RESULTS

Figure 2 shows the normalized endmember spectra used in the unmixing algorithms. As explained in the methodology section above, these spectra are normalized with respect to the maximum value of all the endmembers which was achieved by OA.

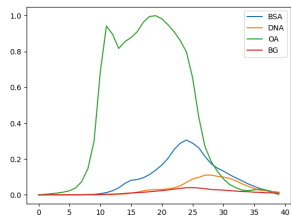


Fig. 2. The four normalized endmembers.

Figure 3 is a visualization of the abundances of BSA, DNA, and OA produced by SciPy's optimizer as the RGB channels

respectively. Figure 4 is an isolation of the green channel. We have increased its brightness for the ease of viewing.

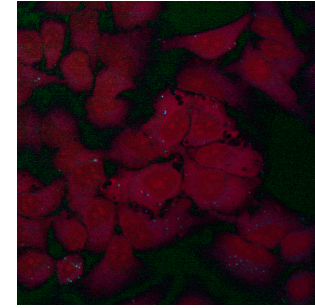


Fig. 3. SciPy LSQ unmixing result of the SRS image of HeLa cells.

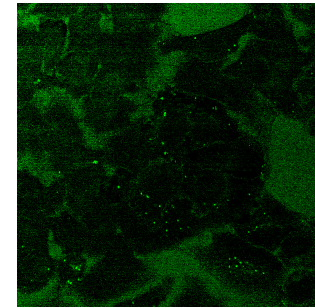


Fig. 4. The green (DNA) channel of SciPy LSQ unmixing result.

Figure 5 is a visualization of the abundances of BSA, DNA and OA produced by the autoencoder neural network as the RGB channels respectively. Figure 6 is an isolation of the green channel of the image in Figure 5. Figure 7 shows an example reconstruction of a cell nuclei pixel by the autoencoder. The endmember spectra, scaled by their presumed abundance values, are shown to display how the reconstruction was conducted.

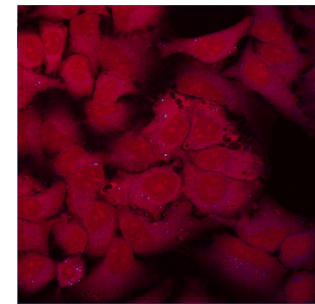


Fig. 5. The initial modified autoencoder unmixing result

IV. DISCUSSION

A. Discussion of SciPy Optimizer Unmixing

In Figure 3 we see that the SciPy optimizer correctly made the lipid droplets almost purely blue (recall this implies high abundance of OA endmember spectrum in the pixel reconstruction) which makes biological sense because lipid droplets

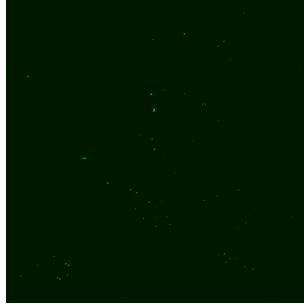


Fig. 6. The DNA channel of autoencoder unmixing result.

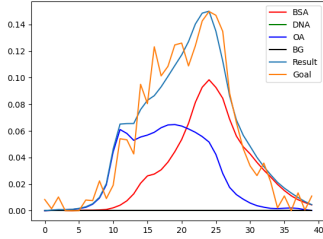


Fig. 7. The autoencoder reconstruction of a cell nuclei pixel.

are composed almost entirely of fatty acids and contain no protein or DNA. When we look at the red channel, we see that the cell body and cell nuclei have high red values which also makes biological sense as both the cell body and nuclei have large amounts of protein. The green channel however is not biologically justified. Isolating this channel (Figure 4), we see that the optimizer used little to no amount of the DNA endmember to reconstruct the nuclei pixels and instead used it mostly in lipid droplet, background and cell body pixels. We would expect the green channel to be present the most in the cell nuclei pixels which is not what we see in Figure 4. We hope that we can tune the autoencoder to the point that we see improvement in the DNA channel.

B. Discussion of Autoencoder Neural Network Unmixing

As for the initial results of the autoencoder, we see that it was equally effective at getting scientifically justifiable abundances of OA in lipid droplet pixels and BSA in cell body and nuclei pixels. However, we seem to be just as ineffective at correctly identifying the abundance of DNA in key regions as the SciPy optimizer. As shown in Figure 6, the autoencoder only assigned noticeable abundance values of the DNA endmember to lipid droplet pixels. This result is not biologically accurate as lipid droplets should show no traces of DNA. Figure 7, which is a sample reconstruction of a cell nuclei pixel, seems to show, however, that the neural network is finding a combination of endmembers that is producing an accurate, in terms of loss function, result. Figure 8 shows the average spectra for each of our three key components. Upon inspection, we see that the noise in the data is making the cell nuclei pixel spectrum look more like the average cell

body pixel as opposed to the average cell nuclei pixel. A reduction of the noise in the data may prove to increase our input data's representation of the difference in spectral shape between cell body and cell nuclei clearly seen in Figure 8. In this regard, noise reduction is needed to improve the accuracy of the model.

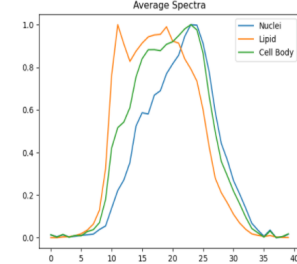


Fig. 8. The average spectra of key component pixels.

V. CONCLUSION

The initial results of the autoencoder are quite similar to those of SciPy's optimizer. Our hypothesis is that noise in the data is increasing the number of "low loss" reconstructions of the input spectrum and thus making it difficult for the neural network to find the biologically accurate one. We believe that reducing the noise of the data may allow the neural network to out perform the LSQ unmixing algorithm. Our current plan is to change how data is fed into the network both during training as well as testing. Instead of feeding in a singular pixel we plan to average the spectra of a 3 pixel by 3 pixel region in an effort to get a spectrum that is closer to the average spectrum of its corresponding component. Although this may reduce the accuracy of our unmixing at the edges of our components, we believe that the overall reduction of noise will help the network identify true linear combination of a majority of the pixels and thus outperform SciPy's Least Square Error optimizer unmixing.

REFERENCES

- [1] E. Jones, T. Oliphant, P. Peterson *et al.*, "SciPy: Open source scientific tools for Python," 2001-. [Online]. Available: <http://www.scipy.org/>
- [2] B. Palsson, J. Sigurdsson, J. R. Sveinsson, and M. O. Ulfarsson, "Hyperspectral unmixing using a neural network autoencoder," *IEEE Access*, vol. 6, pp. 25 646–25 656, 2018.
- [3] J.-X. Cheng and X. S. Xie, "Vibrational spectroscopic imaging of living systems: An emerging platform for biology and medicine," *Science*, vol. 350, no. 6264, 2015.
- [4] F.-K. Lu, S. Basu, V. Igras, M. P. Hoang, M. Ji, D. Fu, G. R. Holtom, V. A. Neel, C. W. Freudiger, D. E. Fisher *et al.*, "Label-free dna imaging in vivo with stimulated raman scattering microscopy," *Proceedings of the National Academy of Sciences*, vol. 112, no. 37, pp. 11 624–11 629, 2015.
- [5] Y. Yuan, N. Shah, M. I. Almohaisin, S. Saha, and F. Lu, "Assessing fatty acid-induced lipotoxicity and its therapeutic potential in glioblastoma using stimulated raman microscopy," *Scientific reports*, vol. 11, no. 1, pp. 1–14, 2021.
- [6] A. Paszke, S. Gross, F. Massa, A. Lerer, J. Bradbury, G. Chanan, T. Killeen, Z. Lin, N. Gimelshein, L. Antiga, A. Desmaison, A. Kopf, E. Yang, Z. DeVito, M. Raison, A. Tejani, S. Chilamkurthy, B. Steiner, L. Fang, J. Bai, and S. Chintala, "Pytorch: An imperative style, high-performance deep learning library," pp. 8024–8035, 2019. [Online]. Available: <http://papers.neurips.cc/paper/9015-pytorch-an-imperative-style-high-performance-deep-learning-library.pdf>